Journal of Marine Science and Technology

Volume 13 | Issue 2 Article 9

A RESEARCH COMBINES NONDESTRUCTIVE TESTING AND A NEURO-FUZZY SYSTEM FOR EVALUATING RIGID PAVEMENT FAILURE POTENTIAL

Shuh-Gi Chern
Professor, Department of Harbor and River Engineering, National Taiwan Ocean University, Keelung, Taiwan 202, R.O.C., sgchern@mail.ntou.edu.tw

Yu-Shih Lee
Ph.D. Candidate, Department of Harbor and River Engineering, National Taiwan Ocean University, Keelung, Taiwan 202, R.O.C

Rong-Feng Hu
Assistant Professor, Department of Air Transportation, Kainau University, Luzhu Taoyuan, Taiwan 338, R.O.C

Yen-Jen Chang
Graduate Student, Department of Harbor and River Engineering, National Taiwan Ocean University, Keelung, Taiwan, R.O.C.

A RESEARCH COMBINES NONDESTRUCTIVE TESTING AND A NEURO-FUZZY SYSTEM FOR EVALUATING RIGID PAVEMENT FAILURE POTENTIAL

Acknowledgements

The authors would to thank the supports of the Chiang Kai-Shek International airport authority for their data and serves that were used in this research.

A RESEARCH COMBINES NONDESTRUCTIVE TESTING AND A NEURO-FUZZY SYSTEM FOR EVALUATING RIGID PAVEMENT FAILURE POTENTIAL

Shuh-Gi Chern*, Yu-Shih Lee**, Rong-Feng Hu***, and Yen-Jen Chang****

Key words: non-destructive testing (NDT), heavy-falling weight deflectometer (HWD), pavement condition index (PCI), neuro-fuzzy system.

ABSTRACT

In recent years, advances in hardware and software technology had brought to significant improvement of NDT (Non-Destructive Test) equipment. In the field of evaluation and designs for the airfield pavement, NDT has been extensively used. NDT is an efficient methodology for assessing the structural condition of an airfield pavement, in the meantime, engineers need to carry other methods for assessing pavement performance, such as visual condition, roughness, and friction characteristics in completing the overall pavement evaluation. In this research, a model combined neuro-fuzzy system, PCI method (pavement condition index, visual inspection) and NDT (Heavy Falling Weight Deflectometer, HWD, structural condition) data are used to evaluate an airfield pavement potential distress. With the help of case studies, it is shown that the proposed model is capable to predict possible area of pavement damage potentials.

INTRODUCTION

Before NDT technology had been developed, pavement structural data must be obtained from many borings, cores, and excavation pits on an existing airfield pavement, those works will be disruptive to airport operations. For example, to conduct a plate load test in order to get in-situ modulus of subgrade reaction *k* of a jointed plain Portland Cement Concrete (PCC), it needs a 1.2 m by 1.8 m pits, and needs to remove each pavement layer until the subgrade is exposed. After the plate-bearing test is completed, it would then need to spend a lot of money to repair the test pit, and may keep the test area closed for several days [13, 24]. In recent years, advances in hardware and software technology had brought to significant improvement of NDT (Nondestructive test) equipment. And NDT has been extensively used in the field of evaluation and designs for the highways and airfield pavement [2, 4-7, 15, 18, 19, 23, 25, 26]. There are many advantages in using NDT which could replace or supplement traditional destructive tests in the airfield, under close contact with Air Traffic Control, it will then eliminate the interference with the operation of airport. The record shows that NDT (FWD) operation can obtain in-situ structural data within 2 to 3 minutes. On regular highway (mainly with Asphalt Concrete pavement) may collect FWD data up to 250 locations per day.

HWD testing is an efficient methodology for assessing the structural condition of an airfield pavement, in the meantime, engineers need to carry other methods for assessing pavement performance, such as PCI (Pavement Condition Index) [3, 11, 21], GPR (Ground Penetrating Radar) [25, 26], roughness, and friction characteristics in completing the overall pavement evaluation. PCI method was widely used in the earlier stage to evaluate the pavement condition. However, limitation of PCI data is that the systems have a tendency to determine PCI values which does not really describe the distress type during visual inspection procedures, as is well known, it is possible to have two pieces of pavement with the same PCI value, but totally different distress types.

For developing a pavement maintenance and rehabilitation strategy, the correlation between structural and functional performances is important. For example, due to environmental distress, a pavement may have a low PCI value, but it still has sufficient strength to accommodate structural loading. It would be essential

Paper Submitted 05/12/04, Accepted 06/01/04. Author for Correspondence: Shuh-Gi Chern. E-mail: sgchern@mail.ntou.edu.tw.

**Professor, Department of Harbor and River Engineering, National Taiwan Ocean University, Keelung, Taiwan 202, R.O.C.*

***Ph.D. Candidate, Department of Harbor and River Engineering, National Taiwan Ocean University, Keelung, Taiwan 202, R.O.C.*

****Assistant Professor, Department of Air Transportation, Kainau University, Luzhu Taoyuan, Taiwan 338, R.O.C.*

*****Graduate Student, Department of Harbor and River Engineering, National Taiwan Ocean University, Keelung, Taiwan, R.O.C.*

to cross check the NDT (FWD) data with PCI value, so as to determine the structural analysis when maintenance works are necessary. A pavement having load related distress would then be repaired with structural overlay or re-construction; and a pavement with severe raveling without load related damage could have a patching, seal coat or minor overlay. An efficient pavement management not only makes engineering progresses but also economic savings.

Because of the wide range of pavement types, loading and local environmental conditions, there are so many parameters influence the pavement performance, it seems that a neuro-fuzzy system may solve this complex problems. In fact, the neuro-fuzzy system had successfully to analysis different problems in civil engineering field, such as the driven piles [1], the stress-strain modeling of sands [10], the liquefaction potential [8, 12, 17, 22] and the slope failure potential [16, 20].

In this research a neuro-fuzzy system is attempted to solve this problems, the PCI investigating record data as well as Heavy-Falling Weight Deflectometer (HWD) data are used to evaluate pavement strength condition that induced pavement damage potentials. In the case study, it is shown that the proposed model is able to predict pavement damage potentials.

OVERVIEW OF NEURAL NETWORKS

A neural network consists of a number of interconnected proceeding units commonly referred to as neurodes or neurons. Each neuron receives an input signal from neurons to which it is connected. Each of these connections has numerical weights associated with it. These weights determine the nature and strength of the influence between the interconnected neurons. The signals from each input are then processed through a weighted sum of the inputs, and the processed output signal is then transmitted to another neuron via a transfer or activation function. A typical transfer function is the sigmoid transfer function. The sigmoid function modulates the weight sum of the inputs so that the output approaches unity when the input gets larger and approaches zero when the input gets smaller.

Figure 1 shows the architecture of a typical neural network consisting of conventional three layers of interconnected neurons. Each neuron is connected to all the neurons in the next layer. There is an input layer that holds the response of the network to the input. It is the intermediate layers, also known as hidden layers that enable these networks to respect and compute complicated associations between patterns. A single hidden layer is common used in most conventional neural networks.

Training of the neural network is essentially carried out through the presentation of a series of example patterns of associated input and output values. The neural network learns what it is to compute through the modification of the weight of the interconnected neurons. Among many learning systems, back-propagation model is the most commonly used one. The learning algorithm processes the patterns in two stages. In the first stage, the input pattern generates a forward flow of signals from the input layer to the output layer. The error of each output neuron is then computed from the difference between the computed and the desired output. The second stage involves the readjustment of the weights in hidden and output layers to reduce the difference between the actual and desired output. Training is carried out iteratively until the root mean squared errors (RMSE) over all training patterns are minimized.

Once the training phase is computed satisfactorily, verification of the performance of the neural network is then carried out the using patterns that were not included in the training set. It will then determine the quality of the predictions in comparison to the desired outputs. This is often called the testing phase. No additional learning occurs during this phase.

Before presenting the input patterns to the neural network, some preprocessing of the data is necessary. This usually involves scaling or normalization of the input patterns to values in the range 0 to 1. This is required because the sigmoid transfer function modulates the output to values between 0 and 1.

1. The structure of neuro-fuzzy system

Figure 2 shows the structure of fuzzy system, consisting of fuzzification, fuzzy rule base, fuzzy infer-

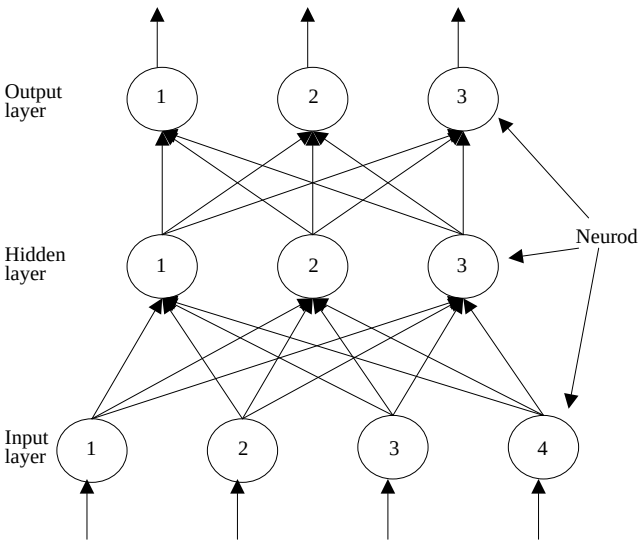

Fig. 1. Typical neural-network architecture.

ence engine and defuzzification function systems in this paper. Figure 3 shows the structure of neuro-fuzzy system in this research, using Fuzzy C-Means (FCM) algorithm to extract the fuzzy rule and divide input patterns into similar clusters, and finds the prototype, i. e. cluster center. Each cluster in this system will map to a relative subnetwork, and the membership function is used to examine the degree of membership between each cluster and pattern. If the degree of membership is over the threshold, then the subnetwork will be fired. If there were many different subnetworks actived at the same time, all of the actived subnetworks were fired. Finally, we use the weighted average method to defuzzy, and use hyperbolic tangent function to transfer output value between –1 to 1.

2. Fuzzy rule

The fuzzy rule can be presented by Equation (1)

IF x_j is v_1 THEN $y = NN_1$

IF x_j is v_2 THEN $y = NN_2$

.

.

.

IF x_j is v_c THEN $y = NN_c$ (1)

where x_j is input vector, $x_j = [x_j^1, x_j^2, \cdots, x_j^n]$, v_c is the prototype of cluster c, $v_c = [v_c^1, v_c^2, \cdots, v_c^n]$, and NN_c is the neuro network relative to cluster c.

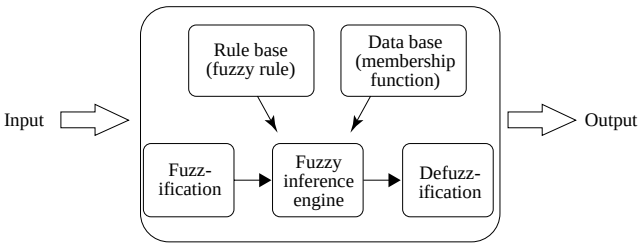

Fig. 2. Typical structure of fuzzy system.

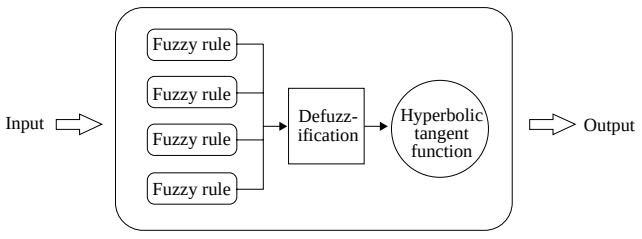

Fig. 3. Structure of neuro-fuzzy system.

3. Determine the cluster center and membership matrix

The FCM algorithm determines the cluster center and membership matrix U using the following steps [14]:

Step 1 Initialized the membership matrix U with a random values between 0 and 1 such that constraints in Equations (3) to (5) are satisfied.

$$U = [u_{ij}]_{i = 1, \ldots, c;\ j = 1, \ldots, n} \tag{2}$$

$$\sum_{i=1}^{c} u_{ij} = 1, \text{ for } j = 1, 2, \ldots, n. \tag{3}$$

$$0 < \sum_{j=1}^{n} u_{ij} < n, \text{ for } i = 1, 2, \ldots, c. \tag{4}$$

$$u_{ij} \in [0, 1], \text{ for } i = 1, \ldots, c;\ j = 1, \ldots, n. \tag{5}$$

where c, i are number of cluster, n, j are number of element, and u_{ij} is degree of membership, between element x_j and cluster i.

Step 2 Calculate the fuzzy cluster center

$$v_i = \frac{1}{\sum_{j=1}^{n} (u_{ij})^m} \sum_{j=1}^{n} (u_{ij})^m x_j, \text{ for } i = 1, 2, \ldots, c. \tag{6}$$

where the v_i is the cluster center, x_j, input vector.

Step 3 Calculate the objective function according Equation (6). Stop the iteration if its improvement over previous iteration is small than a certain threshold or a certain tolerance value

$$J(u_{ij}, v_i) = \sum_{i=1}^{c} \sum_{j=1}^{n} (u_{ij})^m \left\| x_k - v_i \right\|^2 \tag{7}$$

where $m \in [1, \infty]$ is a weight exponential, v_i is the cluster center. $\|\bullet\|$ is Euclidean metric.

Step 4 Compute a new membership function U. Go to Step 2

$$u_{ij} = \frac{1}{\sum_{k=1}^{c} \left(\left\| x_j - v_i \right\|^2 / \left\| x_j - v_k \right\|^2 \right)^{\frac{1}{m-1}}},$$

$$\text{for } i = 1, 2, \ldots, c;\ j = 1, 2, \ldots, n. \tag{8}$$

In this research we use the FCM function in the fuzzy logic toolbox of Matlab.

4. Defuzzification

After clustering procedure, the input vectors divide into different subnetworks. As shown in Figure 4, the subnetwork contains one hidden layer, a logic function works here as an activation function. Using a defuz-

zification process, a fuzzy system transfers the input (fuzzy set) to a crisp output value. The defuz-zification uses the following steps:

Step 1 Calculate the fired value of neurons at hidden layer, and outputs of neurons in hidden layer.

$$v_j(n) = w_{ji}(n)x_i(n) \tag{9}$$

$$y_j(n) = f_j(v_j(n)) = \frac{1}{1+\exp(-v_j(n))} \tag{10}$$

where v_j is fired value of neurons in hidden layer, w_{ji} is the weight between input layer and hidden layer, x_i is output of input layer, y_j is output of neuron, and $f_j(.)$ is a logic function.

Step 2 Calculate the fired value of neurons at output layer, and outputs of neurons in output layer.

$$v_k(n) = w_{kj}(n)y_j(n) \tag{11}$$

$$y_k(n) = f_k(v_k(n)) = v_k(n) \tag{12}$$

where v_k is fired value of neurons in output layer, w_{kj} is the weight between output layer and hidden layer, and y_k is output value of the output layer, and $f_k(\bullet)$ is linear activation function

Step 3 In the output layer, use the weighted average method to together those output value from all subnetwork.

$$\hat{v}(n) = \frac{\sum_{p=1}^{c} m_p \cdot y_{kp}(n)}{\sum_{p=1}^{c} m_p} \tag{13}$$

where $\hat{v}(n)$ is the defuzzification value in the output layer, p is P_{th} fuzzy rule, c is the total number of fuzzy rule, y_{kp} is output value of the P_{th} fuzzy rule, and m_p is the degree of membership that is greater than the vigilance value of P_{th} fuzzy rule.

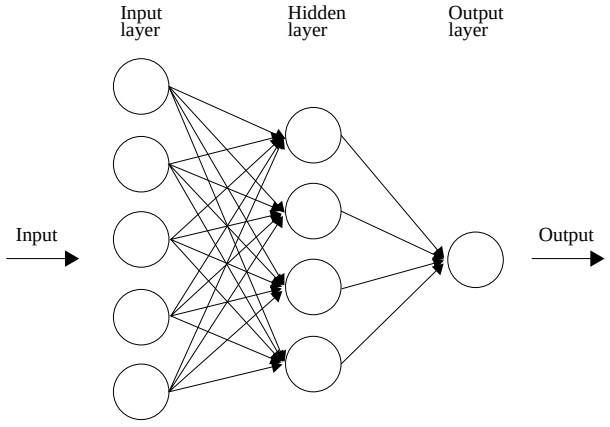

Fig. 4. Structure of subnetwork.

Step 4 Use hyperbolic tangent function transfers output value between –1 to 1.

$$\hat{y}(n) = \hat{f}(\hat{v}(n)) = \frac{\exp(\hat{v}(n)) - \exp(-\hat{v}(n))}{\exp(\hat{v}(n)) + \exp(-\hat{v}(n))} \tag{14}$$

where $\hat{f}(\cdot)$ is the hyperbolic tangent function.

5. Learning in subnetwork

Each subnetwork learns with a least-mean-squared (LSM) method or delta rule, in this paper the weights are updated to minimize the mean-squared error between the actual output and the desired output, the objective function is:

$$E(n) = \frac{1}{2}[y(n) - \hat{y}(n)]^2 \tag{15}$$

where y is the desired output, $\hat{y}$ is the network output signal.

The learning algorithm is described in the following steps:

Step 1. Initialized the weights with small random values.

Step 2. Update the weight in output layer of subnetwork.

$$\Delta w_{kj}(n) = -\eta \cdot \frac{\partial E(n)}{\partial w_{kj}(n)}$$

$$= -\eta \cdot \frac{\partial E(n)}{\partial \hat{y}(n)} \cdot \frac{\partial \hat{y}(n)}{\partial \hat{v}(n)} \cdot \frac{\partial \hat{v}(n)}{\partial y_k(n)} \cdot \frac{\partial y_k(n)}{\partial v_k(n)} \cdot \frac{\partial v_k(n)}{\partial w_{kj}(n)}$$

$$= -\eta \cdot [-(y(n) - \hat{y}(n))] \cdot (1 - \hat{y}^2)) \cdot \frac{m_p}{m_1 + m_2 + \cdots m_c}$$

$$\cdot 1 \cdot y_j(n) \tag{16}$$

where η is learning parameter, n is iterative number, m_p is the degree of membership that is greater than the vigilance value of the p_{th} fuzzy rule, c is the total number of fuzzy rule, y_j is output value of the hidden layer of subnetwork.

Step 3. The weight update of subnetwork hidden layer

$$\Delta w_{ji}(n) = -\eta \cdot \frac{\partial E(n)}{\partial w_{ji}(n)}$$

$$= -\eta \cdot \frac{\partial E(n)}{\partial \hat{y}(n)} \cdot \frac{\partial \hat{y}(n)}{\partial \hat{v}(n)} \cdot \frac{\partial \hat{v}(n)}{\partial y_k(n)} \cdot \frac{\partial y_k(n)}{\partial v_k(n)} \cdot \frac{\partial v_k(n)}{\partial y_j(n)}$$

$$\cdot \frac{\partial y_j(n)}{\partial v_j(n)} \cdot \frac{\partial v_j(n)}{\partial w_{ji}(n)}$$

$$= -\eta \cdot [-(y(n) - \hat{y}(n))] \cdot (1 - \hat{y}^2(n))$$

$$\cdot \frac{m_p}{m_1 + m_2 + \cdots m_c} \cdot 1 \cdot w_{kj}(n) \cdot [y_j(n)$$

$$\cdot (1 - y_j(n))] \cdot x_i(n) \quad (17)$$

where w_{kj} is the weight between output layer and hidden layer, and x_j is input value of the subnetwork. In the back-propagation neural network we use a local gradient parameter δ to modify the weight.

$$\Delta w_{kj}(n) = \eta \bullet \delta_k(n) \bullet y_j(n) \quad (18)$$

$$\Delta w_{ji}(n) = \eta \bullet \delta_j(n) \bullet x_i(n) \quad (19)$$

$$\delta_k(n) = [y(n) - \hat{y}(n)] \cdot (1 - \hat{y}^2(n)) \cdot \frac{m_p}{m_1 + m_2 + \cdots m_c} \quad (20)$$

$$\delta_j(n) = [y(n) - \hat{y}(n)] \cdot (1 - \hat{y}^2(n)) \cdot \frac{m_p}{m_1 + m_2 + \cdots m_c} \bullet [y_j(n) \bullet (1 - y_j(n))]$$

$$= d_k(n) \bullet w_{kl}(n) \bullet [y_j(n) \bullet (1 - y_j(n))] \quad (21)$$

OVERVIEW OF NDT

1. Categories of NDT equipment

Nondestructive testing equipment for airport pavements can be broadly classified as nondeflection and deflection testing equipment [24]. Nondeflection measuring equipment includes ground-penetrating radar, infrared thermography, dynamic cone penetrometer, and devices that measure surface friction, roughness, and surface waves. Deflection measuring equipment can be broadly classified as static or dynamic loading devices. Static loading devices are such as Benkelman Beam and other types of plate bearing tests. Dynamic loading equipment can be further classified to vibratory and impulse devices. Steady-state vibratory devices are including Dynaflect and Road Rater. Impulse load devices are such as the FWD or Heavy- Falling Weight Deflectometer (HWD). The manufacturers including KUAB America, Dynatest Group, Phoenix Scientific Inc., Foundation Mechanics Inc., and Viatest. The impulse load devices are most popular and widely used in the world.

2. Theory of heavy-falling weight deflectometer

Early use of deflection data typically involved consideration of maximum deflection directly under the load, relative to experimental standards. Usually some statistical measure of deflections on a pavement section is compared with an "allowable" deflection level for that section under the expected traffic.

The HWD equipment measures pavement surface deflections from an applied dynamic load that simulates a moving wheel, pavement deflections are recorded directly beneath the load plate and the outermost sensor provides an indication of subgrade strength data. The moduli derived in this way are considered representative of the pavement response to load, and can be used to calculate stresses or strains in the pavement structure for analysis purposes. Calculations of theoretical deflections, and the subsequent stress or strain calculations, currently typically involve linear elastic theory. Empirical use of deflection basin data usually involves one of the "basin parameters" which combine some or all of the measured basin deflections into a single number.

Application of elastic theory may be through the use of:

1. Traditional layered elastic programs based on numerical integration procedures such as ELSYM5, CHEVRON (various versions), BISAR and WESLEA.
2. The Odemark-Boussinesq transformed section approach rather than numerical integration.
3. Finite element programs, either those that have been specifically oriented towards pavement analysis, such as ILLI-PAVE or MICHPAVE, or general structural analysis programs such as SAP (various versions), ANSYS, ABACUS, ADINA, etc.
4. Plate theory such as the Westergaard solutions for PCC pavements.

3. Impulse stiffness modulus

Pavement stiffness is defined as the dynamic force divided by the pavement deflection at the center of the load plate.

$$I(D)SM = \frac{L}{d_o} \quad (22)$$

Where $I(D)SM$ is impulse (dynamic) stiffness modulus (kips/inch), L is applied load (kips) and d_0 is maximum deflection of load plate (inches).

4. Back-calculation

Structural evaluation of pavement deflection response using Non-Destructive Test (NDT) data has been growing since the introduction of the Benkelman Beam at the WASHO Road Test in the early 1950's. Developments in analytical techniques, coupled with improved deflection measurement capabilities, have resulted in the current so-called back-calculation techniques widely employed in pavement evaluation [9, 24].

Briefly, the back-calculation procedure involves calculation of theoretical deflections under the applied

load using assumed pavement layer modulus. These theoretical deflections are compared with measured deflections and the assumed modulus are then adjusted in an intricate procedure until theoretical and measured deflection basins match acceptably well.

Since empirical rules are difficult to generalize across a wide range of pavement types, loading and local environmental conditions, newly developed software tend to reduce the reliance on empirical approaches. Instead, pavements can be analyzed like most other civil engineering structures, i.e., through the use of calculated and allowable stresses and strains at critical points within the pavement structure, under load. The relationships between allowable stresses and strains, and pavement distress, remain essentially empirical. The calculation of existing stresses and strains within the pavement structure can be accomplished through an analytical or mechanistic approach.

5. PCC joints analysis

It is very important to analyze the load transfer efficiency between adjacent PCC slab joints, because the load transfer efficiency can significantly impact the structural capacity of the pavement. In this paper equation has been adopted to define deflection load transfer efficiency.

$$LTE_{\Delta} = \left(\frac{\Delta_{unloaded\_slab}}{\Delta_{loaded\_slab}} \right) 100\% \tag{23}$$

Where LTE_{Δ} is deflection load transfer efficiency (percent), Δ_{loaded_slab} is deflection on loaded slab normally under load plate (mils), and $\Delta_{unloaded\_slab}$ is deflection on adjacent unloaded slab (mils).

CASE STUDIES

In this research, HWD test data were collected using the equipment made by Dynatest Group, and a back-calculation program Elmod 4.5 was adopted for data analysis. Total 331 records combined HWD test and PCI investigation were used in the case study, 280 of these case records are used for the training case, and 51 for the testing phase. Details are shown in Table 1 and 2, respectively, input parameters include layer thickness of PCC, thickness of subbase, ISM, *E* modulus of PCC, *E* modulus of subbase, *E* modulus of subgrade, subgrade reaction at center, subgrade reaction at corner, joint load transfer, and pavement surface condition. As shown in Table 3, there are 12 types of pavement surface distress, in this research we set the input value equal 1 when the pavement surface exists any surface distress. A hyperbolic tangent function transfers output value between −1 to 1, the value −1 means the pavement condition is well, and value 1 means the pavement slab has some problem about cracks, distress of joint, or distress of surface.

The results of the predications using this neuro-fuzzy system would have been tabulated in Table 1 and 2 alongside the actual field performance, the training rate and learning curve are shown in Figures 5 and 6 individually. There are 28 errors in the training data and 16 errors in testing data (90% success rate in training and 68.6% success rate in testing, overall 86.7%, as shown at Table 4). This indicates that the present neuro-fuzzy system with the ability for evaluating pavement failure potential.

CONCLUSION

For developing a pavement maintenance and rehabilitation strategy, the correlation between structural and functional performances is important. For example, due to environmental distress, a pavement may have a low PCI value, but it still has sufficient strength to accommodate structural loading.

In this research a neuro-fuzzy system network has been used to model the complex relationship between rigid pavement, subbase, subgrade, joint load transfer, and in-situ condition, and 90% success rate in training and 68.6% success rate in testing, overall 86.7%. In the Table 4 we find the error rate of "predicting to damage but actually not" significant increase in testing phase, but the locations are random distributed in the airport area, as shown in Figure 7. In this research, we have 10 input parameters but only have 240 training records, it seems that in the future research needs more training

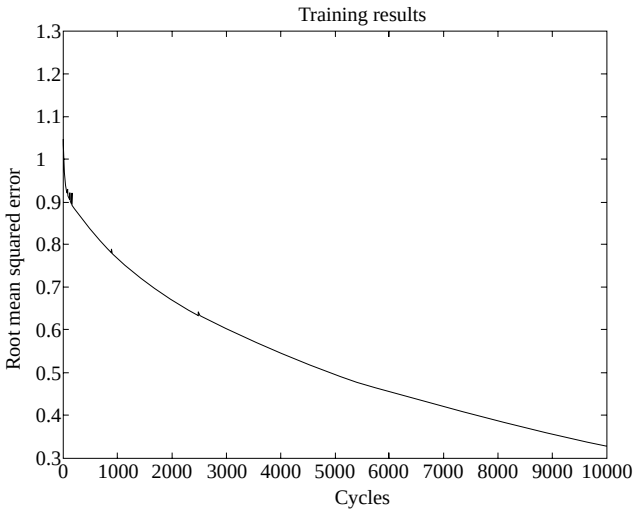

Fig. 5. Learning curve of neuro-fuzzy system.

Table 1. Field behavior data for training set

(1: damage, –1: no damage) The shadow determinates the error of prediction

No.	Layer thickness (mm)		ISM	E modulus (Mpa)			Subgrade reaction (kPa/ mm)		Load transfer	Field behavior	Trainning result
	PCC	Subbase	(kN/mm)	Concrete	Subbase	Subgrade	kc	kj	(%)		
1	380	200	930	18356	949	427	91	168	98.4	1	0.775
2	380	200	1251	34746	565	473	77	73	27.2	1	0.767
3	380	200	1042	32600	451	329	77	78	28.0	1	0.762
4	380	200	1160	48381	779	323	64	52	54.8	1	0.909
5	380	200	921	29700	566	257	64	42	17.3	-1	-0.576
6	410	200	1227	32588	456	354	87	42	88.5	1	0.192
7	380	200	1104	32496	595	327	84	43	70.9	1	-0.223
8	380	200	1222	30825	604	547	108	117	51.9	1	0.843
9	380	200	888	19863	935	370	66	61	68.5	1	0.298
10	380	200	922	25093	1182	213	67	28	5.8	1	0.661
11	380	200	834	23063	722	244	63	45	25.1	1	0.319
12	380	200	1021	31155	563	307	75	14	51.6	-1	-0.861
13	380	200	990	32353	420	278	69	44	15.7	1	0.661
14	380	200	1126	38278	592	382	76	89	95.3	1	0.681
15	380	200	1126	29003	629	410	100	100	95.6	1	0.716
16	380	200	1123	29751	502	410	95	82	95.5	1	0.889
17	410	200	1339	31613	620	436	103	26	69.6	-1	-0.601
18	410	200	1061	30366	376	333	71	117	98.6	-1	0.057
19	410	200	1007	27064	388	341	71	133	97.4	-1	-0.309
20	410	200	932	22367	472	334	70	85	97.2	1	0.644
21	380	200	956	33081	359	333	66	45	85.7	-1	-0.986
22	380	200	1090	35734	578	261	76	45	85.9	1	0.208
23	380	200	1149	35597	550	328	85	81	73.4	1	-0.843
24	380	200	1021	29378	517	381	80	75	93.9	1	-0.290
25	380	200	1032	32372	564	298	74	86	91.5	1	0.875
26	380	200	1099	33575	578	324	81	105	97.8	1	-0.772
27	380	200	1098	33256	483	319	84	108	91.3	1	-0.172
28	380	200	1021	31747	461	293	76	120	96.8	1	0.019
29	380	200	928	31008	732	237	60	119	97.6	-1	-0.957
30	380	200	1026	31087	431	293	78	140	97.8	1	0.120
31	380	200	976	31485	608	273	67	123	95.1	1	-0.586
32	380	200	1005	34808	395	284	69	127	96.6	-1	-0.851
33	380	200	906	33266	376	242	59	77	97.5	-1	-0.963
34	380	200	1067	33945	405	285	79	58	87.3	-1	-0.671
35	380	200	1105	32008	550	317	86	127	94.1	-1	-0.864
36	380	200	1167	34509	485	293	91	138	89.7	-1	-0.860
37	380	200	1237	36383	557	441	96	99	91.8	1	0.367
38	380	200	1293	33714	569	483	112	91	84.0	-1	-0.848
39	380	200	1288	30382	728	596	118	118	81.4	1	0.897
40	380	200	1333	42353	565	462	98	110	91.2	-1	-0.727
41	410	200	1464	32373	381	669	127	166	93.6	1	0.956
42	410	200	1278	29247	718	370	99	63	88.2	-1	-0.829
43	410	200	1058	25823	658	309	76	92	92.4	1	0.075
44	380	200	1089	31388	615	258	84	84	87.6	1	0.608
45	380	200	1103	29790	608	328	90	120	96.5	-1	-0.972
46	380	200	1063	28768	752	288	84	86	78.6	1	-0.469
47	380	200	924	26413	723	234	69	67	93.1	-1	-0.670
48	380	200	1046	28161	743	363	83	117	88.7	-1	-0.731
49	380	200	1050	29069	819	312	80	97	93.3	-1	-0.914
50	380	200	1181	28419	713	528	105	79	84.3	1	0.757
51	380	200	1126	36564	873	289	75	84	92.5	1	0.768

Table 1. Field behavior data for training set (continued)

(1: damage, –1: no damage) The shadow determinates the error of prediction

No.	Layer thickness (mm)		ISM	E modulus (Mpa)			Subgrade reaction (kPa/mm)		Load transfer	Field behavior	Trainning result
	PCC	Subbase	(kN/mm)	Concrete	Subbase	Subgrade	kc	kj	(%)		
52	410	200	1218	21716	573	574	119	143	95.1	-1	-0.744
53	410	200	1461	34639	780	436	110	84	91.0	1	0.705
54	410	200	1306	30603	805	399	98	38	97.9	-1	-0.922
55	410	200	1236	30407	868	369	87	71	80.8	-1	-0.841
56	410	200	1353	35762	674	367	94	80	90.8	-1	-0.952
57	410	200	1109	34168	274	277	72	105	82.4	-1	-0.730
58	410	200	1259	30823	648	438	93	130	95.8	-1	-0.924
59	380	200	1227	33487	495	468	103	88	76.8	-1	-0.796
60	380	200	809	30005	329	225	52	84	84.4	-1	-0.992
61	380	200	996	35195	500	265	65	60	59.2	-1	-0.918
62	380	200	896	26661	410	219	69	64	52.4	-1	-0.665
63	380	200	941	30297	405	314	68	83	89.3	-1	-0.949
64	380	200	996	32492	422	259	71	85	81.3	-1	-0.965
65	380	200	1289	39048	488	350	100	111	50.1	-1	-0.868
66	410	200	1042	36614	438	223	57	51	58.2	1	0.716
67	410	200	939	28729	352	209	53	184	43.2	1	0.788
68	410	200	974	38793	417	175	48	73	84.6	1	0.577
69	410	200	852	33868	406	202	41	32	25.1	1	0.366
70	410	200	965	40650	463	198	44	5	42.5	1	0.677
71	410	200	925	35815	543	183	45	64	55.4	1	0.797
72	410	200	772	26966	382	169	42	59	31.9	1	0.606
73	410	200	744	29352	446	192	36	22	73.1	-1	-0.829
74	410	200	1081	43688	380	196	53	100	93.2	-1	-0.859
75	410	200	1081	43688	380	196	53	100	93.2	-1	-0.859
76	410	200	1151	24455	668	504	95	90	97.3	-1	-0.908
77	380	200	804	31370	589	176	46	74	97.7	-1	-0.997
78	380	200	1011	31907	817	264	66	100	97.4	-1	-0.903
79	380	200	983	28922	577	287	74	113	97.7	-1	-0.759
80	380	200	1056	28716	675	295	84	123	98.0	-1	-0.922
81	380	200	1024	30975	607	256	75	84	98.9	-1	-0.264
82	380	200	1119	33629	761	381	81	102	98.0	-1	-0.928
83	380	200	978	26966	592	299	78	99	96.4	-1	-0.753
84	410	200	1192	29433	796	326	85	95	95.2	-1	-0.997
85	410	200	1098	23523	868	403	86	136	95.3	-1	-0.823
86	410	200	1090	24787	505	466	87	114	98.8	-1	-0.684
87	380	200	1236	43251	607	401	82	117	97.4	1	0.820
88	380	200	1135	30702	705	417	91	140	98.8	1	0.112
89	380	200	1077	37730	426	314	73	107	99.3	-1	-0.743
90	380	200	945	34203	495	246	60	61	94.3	-1	-0.952
91	380	200	1028	33507	525	294	72	86	99.8	-1	-0.815
92	380	200	985	26360	597	360	80	65	97.3	-1	-0.870
93	380	200	1017	27859	531	418	83	105	99.4	-1	-0.836
94	380	200	917	30731	507	242	62	115	97.9	-1	-0.931
95	380	200	979	33815	415	258	67	106	97.1	-1	-0.926
96	380	200	942	29055	482	265	69	89	69.9	-1	-0.949
97	380	200	1130	31965	654	321	88	157	98.2	-1	-0.917
98	380	200	1136	33988	578	309	86	81	73.4	-1	-0.620
99	380	200	1010	32836	455	260	72	84	94.1	1	-0.689
100	380	200	1233	34296	579	445	100	117	70.3	-1	-0.652
101	380	200	1121	36533	573	331	79	77	95.3	-1	0.142
102	380	200	1414	41055	416	511	116	201	94.6	1	0.928

Table 1. Field behavior data for training set (continued)

(1: damage, –1: no damage) The shadow determinates the error of prediction

No.	Layer thickness (mm)		ISM	E modulus (Mpa)			Subgrade reaction (kPa/mm)		Load transfer	Field behavior	Trainning result
	PCC	Subbase	(kN/mm)	Concrete	Subbase	Subgrade	kc	kj	(%)		
103	410	200	1368	32977	541	434	105	166	97.9	1	-0.133
104	410	200	1022	29894	304	270	68	68	17.2	1	-0.069
105	410	200	1167	35244	376	387	75	57	80.6	-1	-0.162
106	380	200	1067	47404	234	328	62	42	84.6	-1	-0.940
107	380	200	1140	38046	268	372	85	76	31.3	-1	-0.663
108	380	200	947	34721	255	312	64	58	27.2	-1	-0.310
109	380	200	957	39439	237	248	59	49	25.2	-1	-0.463
110	380	200	1080	41107	255	290	71	67	24.9	1	0.326
111	380	200	1156	41124	373	319	79	58	23.4	-1	-0.403
112	380	200	752	28611	188	186	49	50	11.2	-1	-0.963
113	380	200	1065	33511	287	429	82	60	53.4	1	0.993
114	380	200	1002	36942	331	326	66	62	22.1	1	0.502
115	380	200	950	37611	219	255	61	56	21.4	-1	-0.611
116	380	200	889	34544	450	215	54	38	19.3	-1	-0.818
117	380	200	1245	42660	347	438	89	39	34.9	1	0.983
118	380	200	1050	38722	297	323	70	46	14.3	1	0.249
119	380	200	965	35437	231	304	66	47	17.3	-1	-0.433
120	380	200	1133	40437	363	300	77	49	14.5	-1	-0.643
121	380	200	1266	43401	439	452	89	45	39.9	1	0.613
122	410	200	1278	42500	339	326	77	38	15.0	-1	-0.952
123	410	200	1207	33324	288	474	87	64	95.7	1	0.960
124	380	200	920	30691	325	312	66	24	48.4	-1	-0.609
125	380	200	1025	36843	318	280	70	65	28.7	1	-0.008
126	380	200	932	37684	216	293	58	34	94.9	-1	-0.997
127	380	200	901	34715	261	220	58	47	14.1	-1	-0.983
128	380	200	1055	37160	363	284	72	78	22.5	-1	-0.061
129	380	200	936	33771	237	225	95	25	57.3	1	0.849
130	380	200	870	30704	327	238	59	48	76.6	-1	-0.871
131	380	200	1000	35424	243	334	70	47	93.3	-1	-0.898
132	380	200	1021	35934	319	290	71	80	96.2	-1	-0.958
133	380	200	1171	42950	339	338	79	84	95.3	1	0.355
134	410	200	1053	27463	381	316	76	86	97.7	1	0.283
135	410	200	1137	33033	296	324	77	53	89.0	-1	-0.437
136	380	200	1130	35264	455	312	85	43	96.0	-1	-0.565
137	380	200	867	31903	532	241	54	61	85.0	-1	-0.995
138	380	200	938	27991	543	255	70	73	40.7	-1	-0.790
139	380	200	1021	30679	502	342	77	45	83.5	1	0.208
140	380	200	470	14440	483	102	32	51	35.6	-1	-0.541
141	380	200	923	27847	557	262	68	77	97.0	1	-0.250
142	380	200	1134	37279	557	308	79	43	59.8	-1	-0.909
143	380	200	1046	34735	470	291	73	42	81.9	-1	-0.749
144	380	200	1199	33865	925	361	90	120	94.5	-1	-0.894
145	380	200	996	29542	281	404	81	67	99.1	-1	-0.616
146	380	200	1252	39966	349	383	95	73	94.6	-1	-0.703
147	380	200	969	23993	1114	282	77	77	20.4	-1	-0.723
148	380	200	1076	36541	145	338	82	62	84.9	1	0.125
149	380	200	898	38474	85	246	57	44	16.0	-1	-0.882
150	410	200	1122	29785	659	353	76	99	96.0	-1	-0.967
151	410	200	1102	28350	694	356	76	123	97.2	-1	-0.812
152	410	200	1017	29949	272	342	68	97	91.9	-1	-0.682
153	410	200	1510	32248	2201	534	108	105	88.5	1	-0.318

Table 1. Field behavior data for training set (continued)

(1: damage, –1: no damage) The shadow determinates the error of prediction

No.	Layer thickness (mm)		ISM	E modulus (Mpa)			Subgrade reaction (kPa/mm)		Load transfer	Field behavior	Trainning result
	PCC	Subbase	(kN/mm)	Concrete	Subbase	Subgrade	kc	kj	(%)		
154	410	200	1097	30673	743	296	70	95	96.8	-1	-0.924
155	410	200	1017	29949	272	342	68	97	91.9	-1	-0.682
156	410	200	1510	32248	2201	534	108	105	88.5	-1	-0.318
157	410	200	1103	28733	424	392	80	137	98.9	-1	-0.970
158	410	200	1135	28740	388	458	85	124	98.3	1	-0.699
159	410	200	1203	36977	324	391	78	79	87.5	1	-0.073
160	410	200	1141	35081	324	369	73	53	95.4	1	-0.264
161	410	200	1164	35535	332	385	73	80	76.5	-1	-0.814
162	410	200	1071	29063	490	362	75	76	72.2	-1	-0.947
163	410	200	1189	35820	340	384	78	51	68.1	1	-0.263
164	410	200	1101	27920	485	407	80	93	82.1	-1	-0.960
165	410	200	489	12504	190	142	36	140	79.9	-1	-0.995
166	410	200	711	16628	197	315	58	56	49.1	1	0.406
167	410	200	879	30443	119	330	54	40	36.9	1	0.785
168	410	200	906	35094	240	232	48	45	78.3	1	0.749
169	410	200	978	36549	253	216	53	55	84.3	-1	-0.389
170	410	200	858	24726	240	280	58	51	44.3	1	0.950
171	410	200	955	34522	171	266	55	43	29.6	1	0.023
172	410	200	1071	46295	215	218	52	45	80.1	1	0.736
173	410	200	756	21452	176	246	53	60	54.3	-1	0.679
174	410	200	952	30278	161	252	62	52	80.1	1	0.772
175	410	200	995	36450	240	252	55	44	77.4	1	0.697
176	410	200	771	28371	386	158	40	23	8.3	-1	-0.821
177	410	200	845	36294	490	177	37	23	53.6	-1	0.159
178	410	200	658	22105	328	220	37	28	35.5	1	0.493
179	410	200	923	44398	466	178	38	28	43.7	1	0.700
180	410	200	767	27660	365	155	41	33	55.1	1	0.224
181	410	200	661	20263	368	163	40	30	68.5	-1	-0.778
182	410	200	769	25348	332	169	44	28	32.9	-1	0.423
183	410	200	677	16999	260	159	50	60	74.6	-1	-0.702
184	410	200	1460	37666	623	433	105	188	94.3	-1	-0.808
185	410	200	1389	47722	583	377	78	100	92.8	-1	-0.834
186	410	200	1204	36195	445	372	77	136	96.8	-1	-0.914
187	410	200	1157	27182	358	491	93	150	98.5	-1	-0.542
188	410	200	1042	32539	509	279	62	121	96.9	-1	-0.646
189	410	200	794	30454	545	198	63	52	99.6	-1	-0.832
190	410	200	1052	31212	371	320	68	121	97.3	1	0.324
191	410	200	1048	31984	446	310	65	116	97.2	1	-0.377
192	410	200	1046	26748	624	361	73	120	96.6	1	-0.544
193	410	200	1148	31924	490	389	77	131	95.1	-1	-0.977
194	410	200	1187	36805	507	369	73	134	97.8	-1	-0.879
195	410	200	910	34700	58	262	53	49	92.3	-1	-0.826
196	410	200	922	45803	4	206	46	26	91.4	1	0.992
197	410	200	923	42009	34	239	47	26	86.4	1	0.964
198	440	300	1121	27245	385	299	137	110	91.8	-1	-0.993
199	440	300	1452	36109	473	478	80	92	95.8	-1	-1.000
200	440	300	1152	25489	429	397	69	102	96.3	-1	-1.000
201	440	300	1112	23294	569	400	66	53	63.1	-1	-1.000
202	440	300	1447	38742	520	487	74	64	88.4	-1	-1.000
203	410	200	1319	28317	1345	333	121	67	48.3	1	0.941
204	410	200	1518	32885	968	466	121	56	52.4	1	0.733

Table 1. Field behavior data for training set (continued)

(1: damage, –1: no damage) The shadow determinates the error of prediction

No.	Layer thickness (mm)		ISM	E modulus (Mpa)			Subgrade reaction (kPa/mm)		Load transfer	Field behavior	Trainning result
	PCC	Subbase	(kN/mm)	Concrete	Subbase	Subgrade	kc	kj	(%)		
205	410	200	1118	28690	1077	309	73	81	90.2	-1	-0.989
206	410	200	1071	40983	11	236	67	96	97.5	-1	-0.976
207	410	200	987	28847	128	292	71	83	95.3	1	0.148
208	410	200	1204	26813	1283	483	87	44	72.7	-1	-0.886
209	410	200	1057	22404	886	251	83	66	84.4	-1	-0.976
210	410	200	1510	35227	1297	326	109	134	93.8	-1	-0.935
211	410	200	831	33174	22	161	49	49	99.5	1	0.953
212	410	200	1028	43289	26	213	69	26	12.6	-1	-0.991
213	410	200	1022	32127	151	327	68	38	82.1	1	0.654
214	410	200	1433	36951	760	399	101	90	69.1	1	0.245
215	410	200	1230	29781	557	418	93	72	78.0	1	-0.387
216	410	200	1194	33115	424	411	82	71	29.5	-1	-0.400
217	410	200	1070	30673	360	297	72	65	17.4	-1	-0.135
218	410	200	1137	32104	482	379	76	77	63.5	-1	-0.887
219	410	200	1180	31577	520	312	82	94	82.2	-1	-0.934
220	380	200	1179	34972	638	307	89	81	86.9	-1	-0.801
221	380	200	1308	44097	574	329	91	84	36.3	-1	-0.988
222	380	200	1526	37634	760	511	137	100	54.2	-1	-0.388
223	380	200	1072	35568	724	298	72	77	84.8	1	-0.049
224	380	200	1209	29125	495	566	113	113	29.1	1	0.771
225	380	200	1265	35163	754	387	100	95	42.8	-1	-0.650
226	380	200	1468	36965	912	398	126	131	83.8	1	0.628
227	410	200	1479	28781	1095	388	127	133	82.4	1	0.777
228	410	200	1532	35282	800	426	119	142	85.9	1	0.872
229	410	200	1548	36716	814	452	117	81	16.1	1	0.909
230	380	200	1051	33191	338	315	80	56	40.0	1	0.272
231	380	200	1314	29777	320	677	137	144	90.1	1	0.970
232	380	200	780	25192	339	198	56	67	89.9	1	0.720
233	380	200	995	33802	342	267	70	68	20.7	1	0.470
234	380	200	1196	35312	678	350	90	84	86.8	-1	-0.907
235	380	200	1177	32570	433	426	99	62	89.6	1	0.701
236	410	200	1166	34224	489	321	75	91	79.3	1	-0.473
237	410	200	1030	28589	428	294	70	86	30.3	-1	-0.288
238	410	200	1051	29556	557	301	68	86	94.6	-1	-0.416
239	410	200	1276	28727	475	407	105	120	34.5	1	0.919
240	410	200	1268	30815	724	508	93	97	70.8	-1	-0.903
241	410	200	1208	40930	659	324	67	54	37.1	1	0.710
242	410	200	1244	30143	725	437	91	83	35.9	-1	-0.332
243	410	200	1254	31465	545	466	92	102	31.5	1	0.140
244	410	200	1319	35266	551	445	92	84	88.7	-1	-0.137
245	410	200	1446	47971	493	436	85	91	70.4	-1	-0.851
246	410	200	1248	31555	365	442	95	116	78.8	-1	-0.647
247	410	200	1365	36351	550	413	96	133	79.7	-1	-0.788
248	410	200	1254	32306	397	497	93	66	94.6	1	0.909
249	410	200	1261	34181	557	361	87	95	76.3	-1	-0.951
250	410	200	1276	28936	850	418	97	98	74.7	1	0.338
251	410	200	1310	38386	586	442	84	88	82.9	1	-0.374
252	410	200	1564	43311	699	638	105	123	71.7	1	0.805
253	410	200	1227	31218	517	395	90	84	67.3	-1	-0.595
254	410	200	1394	51331	421	431	76	125	98.4	1	0.628
255	410	200	1310	47915	605	349	69	118	99.7	1	0.299

Table 1. Field behavior data for training set (continued)

(1: damage, –1: no damage) The shadow determinates the error of prediction

No.	Layer thickness (mm)		ISM	E modulus (Mpa)			Subgrade reaction (kPa/mm)		Load transfer	Field behavior	Trainning result
	PCC	Subbase	(kN/mm)	Concrete	Subbase	Subgrade	kc	kj	(%)		
256	410	200	1533	41559	586	516	107	166	97.5	1	0.847
257	410	200	1378	40614	627	490	88	165	95.9	-1	-0.915
258	410	200	1326	41798	460	477	82	151	98.0	-1	-0.674
259	410	200	1397	42786	436	458	89	138	97.3	1	0.538
260	410	200	1259	35553	550	424	83	172	96.2	-1	-0.962
261	410	200	1484	43043	658	572	96	154	96.7	1	0.921
262	380	200	824	27938	593	202	54	78	81.5	-1	-0.933
263	380	200	1193	39164	585	292	84	97	85.5	-1	-0.405
264	380	200	1022	30203	532	304	78	82	82.3	-1	-0.270
265	410	200	994	23567	443	367	77	99	82.3	-1	-0.702
266	410	200	1197	28099	789	343	89	116	80.4	-1	-0.996
267	410	200	1162	20411	1596	289	99	195	66.1	-1	-0.917
268	410	200	1137	29210	709	288	79	90	77.9	-1	-0.927
269	450	300	1575	31238	735	458	94	90	91.5	-1	-1.000
270	450	300	1084	23582	400	297	62	77	88.4	-1	-1.000
271	450	300	1249	35569	710	395	53	56	47.2	-1	-0.997
272	450	300	1575	31238	735	458	94	90	91.5	-1	-1.000
273	450	300	1102	23925	760	396	57	63	65.7	-1	-0.999
274	450	300	1153	24264	306	447	71	77	90.6	-1	-0.999
275	410	200	1043	39335	543	249	55	37	46.2	-1	-0.190
276	410	200	1133	45290	495	282	56	51	58.0	-1	-0.863
277	410	200	1261	37393	543	408	80	76	51.7	1	0.449
278	410	200	1190	30965	335	470	96	85	47.4	-1	-0.947
279	410	200	1278	32174	461	522	70	69	56.6	-1	-0.737
280	410	200	1203	35592	446	365	78	78	50.7	-1	-0.782

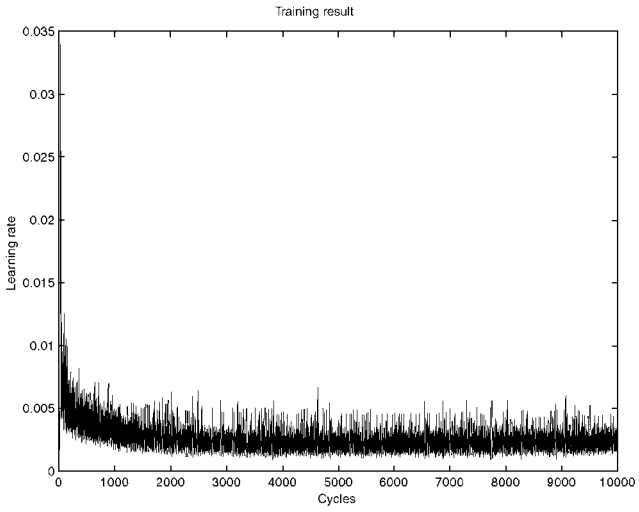

Fig. 6. Learning rate of neuro-fuzzy system.

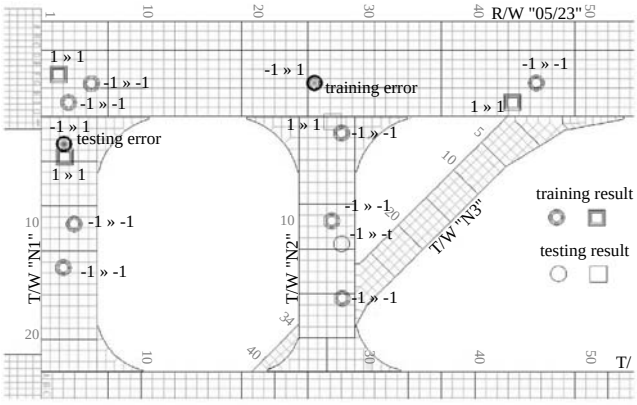

Fig. 7. Part drawing of training and testing results at runway threshold area.

data to improve the accuracy.

Besides those parameters adopted in this paper, the other factors, such as PCC slab warping and curling, moisture contents in each of the layers, voids, loss of support, settlement occurred beneath the pavement layer, all of them also influence the deflection basins and get

Table 2. Field behavior data for testing set

No.	Layer thickness (mm)		ISM	E modulus (Mpa)			Subgrade reaction (kPa/mm)		Load transfer	Field behavior	Testing result
	PCC	Subbase	(kN/mm)	Concrete	Subbase	Subgrade	kc	kj	(%)		
1	380	200	987	28228	484	346	78	66	22.9	-1	-0.437
2	380	200	1288	29697	1047	537	115	34	61.6	1	0.612
3	380	200	1282	40569	590	372	93	61	99.5	-1	-0.517
4	380	200	1115	32380	447	419	89	60	91.1	1	0.981
5	380	200	1161	35303	661	341	85	111	93.7	1	0.129
6	380	200	831	25962	444	233	60	132	95.8	1	-0.922
7	380	200	940	27622	495	277	72	101	98.3	1	-0.496
8	380	200	1316	37401	743	479	103	67	95.2	-1	0.426
9	410	200	1282	34408	432	370	91	124	88.4	-1	-0.784
10	380	200	1058	33227	1098	267	69	95	74.2	-1	-0.951
11	380	200	1108	31757	752	323	84	95	82.6	1	-0.157
12	410	200	1364	29446	627	537	114	93	82.3	-1	0.801
13	410	200	1114	35732	477	282	66	46	97.6	1	0.301
14	410	200	1246	33681	557	347	86	90	92.1	-1	-0.914
15	380	200	960	29527	602	312	69	78	94.0	-1	-0.482
16	380	200	868	25923	356	338	67	80	92.4	-1	-0.661
17	410	200	897	34573	495	172	44	67	48.4	-1	0.844
18	410	200	725	23381	405	176	42	81	95.6	1	-0.949
19	410	200	819	28324	490	188	44	26	86.5	-1	-0.845
20	380	200	1245	43155	705	326	82	125	96.8	-1	0.164
21	380	200	1033	30431	584	276	78	92	98.6	-1	-0.197
22	410	200	1211	29468	490	495	92	90	98.5	-1	-0.075
23	380	200	914	30990	507	275	61	74	95.5	1	-0.820
24	380	200	1215	43938	461	414	80	107	97.8	1	0.927
25	380	200	1087	34502	277	443	84	58	20.3	1	-0.911
26	380	200	1138	39130	340	378	81	60	91.0	1	0.880
27	380	200	1256	41300	340	491	93	57	80.1	1	0.661
28	380	200	972	31452	495	270	69	81	43.0	-1	-0.647
29	380	200	1284	35305	586	462	106	88	42.6	-1	-0.656
30	380	200	1275	38012	1100	366	90	65	97.9	1	0.005
31	410	200	1102	28350	694	356	76	123	97.2	-1	-0.736
32	410	200	1149	33769	357	370	76	129	98.2	-1	-0.896
33	410	200	1111	34446	308	360	72	89	97.0	-1	-0.539
34	410	200	811	26417	184	297	50	46	49.2	1	0.948
35	410	200	912	32664	208	274	52	40	56.5	-1	0.982
36	410	200	767	22944	333	183	48	30	49.3	1	0.738
37	410	200	1384	38776	376	452	99	99	96.2	-1	0.094
38	410	200	1139	35633	388	368	71	116	97.8	1	-0.495
39	440	300	1359	25575	429	573	95	50	91.3	-1	-0.997
40	410	200	1201	30157	235	486	96	98	98.6	1	0.706
41	410	200	1111	30717	802	298	71	69	86.6	-1	-0.572
42	410	200	1307	32072	450	453	101	105	82.1	-1	-0.003
43	380	200	871	33357	208	237	57	52	89.7	-1	-0.897
44	380	200	1154	32167	676	436	91	78	16.9	1	0.889
45	410	200	1382	39941	688	463	88	103	87.3	-1	-0.069
46	410	200	1225	31827	485	347	88	89	65.1	1	-0.850
47	410	200	1165	48652	431	304	55	85	96.9	1	-0.647
48	380	200	1155	35337	550	271	86	111	48.5	-1	-0.651
49	250	200	498	20111	743	197	70	79	76.4	1	-0.917
50	410	200	1183	36243	488	369	73	78	57.2	-1	-0.860
51	410	200	1208	33964	436	397	78	75	57.6	-1	-0.446

Table 3. Error of prediction

	Actual behavior: damage Model prediction: No damage (%)	Actual behavior: No damage Model prediction: damage (%)	Success rate(%)
Training set (113** 167*)	8.2	1.8	90.0
Testing set (22** 29*)	19.6	11.8	68.6

*Actual pavement behavior: no damage
**Actual pavement behavior: damage

Table 4. Pavement surface condition of testing data

No.	Field behavior	Testing result	Longitudinal cracks	Transverse cracks	Corner breaks	Durability cracks	Joint spalling	Pumping sealant loss	Blow-up	Faulting	Polishing	Pothole	Patch
1	-1	-0.437											
2	1	0.612						1					1
3	-1	-0.517											
4	1	0.981											3
5	1	0.129						1					1
6	1	-0.922											2
7	1	-0.496						2					
8	-1	0.426											
9	-1	-0.784											
10	-1	-0.951											
11	1	-0.157											2
12	-1	0.801											
13	1	0.301					1					1	
14	-1	-0.914											
15	-1	-0.482											
16	-1	-0.661											
17	-1	0.844											
18	1	-0.949											1
19	-1	-0.845											
20	-1	0.164											
21	-1	-0.197											
22	-1	-0.075											
23	1	-0.820											1
24	1	0.927											1
25	1	-0.911										1	
26	1	0.880											1
27	1	0.661											1
28	-1	-0.647											
29	-1	-0.656											
30	1	0.005	2										1
31	-1	-0.736											
32	-1	-0.896											
33	-1	-0.539											
34	1	0.948											1
35	-1	0.982					1						
36	1	0.738											
37	-1	0.094											
38	1	-0.495											3
39	-1	-0.997											
40	1	0.706											1
41	-1	-0.572											
42	-1	-0.003											
43	-1	-0.897											
44	1	0.889											1
45	-1	-0.069											
46	1	-0.850							1				
47	1	-0.647											2
48	-1	-0.651											
49	1	-0.917			1		1		2				
50	-1	-0.860											
51	-1	-0.446											

different results. But, in fact, it is not easy to collect those data from all pavement slabs. Such as slab curling occurs due to differences in temperature between the top and bottom of the slab, the slab corners may lift off the base during nighttime curling, and slab center may lift off during daytime curling.

However, it seems the model combing a nondestructive testing and a neuro-fuzzy system is an economical way to evaluate rigid pavement failure potential between the service performance and the structure performance.

ACKNOWLEDGEMENTS

The authors would to thank the supports of the Chiang Kai-Shek International airport authority for their data and serves that were used in this research.

REFERENCES

1. Abu, K.M.A., "General Regression Neural Networks for Driven Piles in Cohesionless Soils," *J. Geotech. Geoenviron.*, Vol. 124, No. 12, pp. 177-1185 (1998).
2. ASTM, "D4695 Standard Test Method of Deflections with a Falling Weight Type Impulse Load Device," Vol. 4.03, Sec. 4, pp. 482-484 (1996).
3. ASTM, "D5340 Standard Test Method for Airport Pavement Condition Index Survey," Vol. 4.03, Sec. 4, pp. 552-599 (1996).
4. ASTM, "Standard Guide for General Pavement Deflection Measurement," D4695-96, pp. 485-487 (1996).
5. Boutros, E.S., Mamlouk, M.S., and Trevor, G.P., "Dynamic Analysis of Falling Weight Deflectometer Data," *Transportat. Res. Rec. 1070*, pp. 63-68 (1986).
6. Bush III, A.J. and Alexander, D.R., "Pavement Evaluation Using Deflection Basin Measurements and Layered Theory," *Transport. Res. Rec. 1022*, pp. 16-29 (1985).
7. Chang, D.W., Kang, V.Y., Roesset, J.M., and Stokoe, K.H., "Effects of Depth to Bedrock on Deflection Basins Obtained with Dynaflect FWD Test," *Transport. Res. Rec. 1355*, pp. 8-16 (1992).
8. Chern, S.G., Hu, R.F., Chang, Y.J., and Tsai, I.F., "Fuzz-ART Neural Networks for Predicting Chi-Chi Earthquake Induced Liquefaction in Yuan-Lin Area," *J. Mar. Sci. Technol.*, Vol. 10, No. 1 (2002).
9. Dater, M.I., Smith, K.D., and Hall, K.T., "Concrete Pavement Backcalculation Results from Field Studies," *Transport. Res. Rec. 1377*, pp. 7-16 (1993).
10. Ellis, G.W., Yao, C., Zhao, R., and Penumadu, D., "Stress-Strain Modeling of Sands Using Artificial Neural Networks," *J. Geotech. Eng.*, Vol. 121, No. 5, pp. 429-435 (1995).
11. Fred, F., "Pavement Management Systems –Past, Present and Future," *Public Roads*, Vol. 62, No. 1, pp. 16-23 (1998).
12. Goh, A.T.C., "Seismic Liquefaction Potential Assessed by Neural Network," *J. Geotech. Eng.*, Vol. 120, No. 9, pp. 1467-1480 (1994).
13. Huang, Y.H., *Pavement Analysis and Design*, Prentice-Hall, Inc., Englewood Cliffs, NJ (1993).
14. Jang, J.S., Sun, C.T., and Mizutani, E., *Neural-Fuzzy and Soft Computing*, Prentice-Hall, Inc., Englewood Cliffs, NJ (1997).
15. Johnson, R.F. and Rish III J.W., "Rolling Weight Deflectometer with Thermal and Vibrational Bending Compensation," *Transport. Res. Rec. 1540*, pp. 77-82 (1996).
16. Juang, C.H., Chen, C.J., and Tien, Y.M., "Appraising CPT-Based Liquefaction Resistance Evaluation Methods: Artificial Neural Networks Approach," *Can. Geotech. J.*, Vol. 36, No 3, pp. 443-454 (1999).
17. Juang, C.H., Lee, D.H., and Sheu, C., "Mapping Slope Failure Potential Using Fuzzy Sets," *J. Geotech. Eng.*, Vol. 118, No. 3, pp. 475-494 (1992).
18. Kulkarni, A.D., *Computer Vision and Fuzzy-Neural Systems*, Prentice-Hall, Inc., Englewood Cliffs, NJ (2001).
19. Mario, S.G. and Jim, W.H., "Comparative Study of Selected Non-destructive Testing Devices," *Transport. Res. Rec. 852*, pp. 32-71 (1974).
20. Ni, S.H., Lu, P.C., and Juang, C.H., "A Fuzzy Neural Network Approach to Evaluation of Slope Failure Potential," *Microcomput. Civil Eng.*, Vol. 11, pp. 59-66 (1996).
21. Schwandt, G., "Airport Pavement Management System Saves Millions," *Public Works*, Vol. 127, No. 1, pp. 53-55 (1996).
22. Tung, A.T.Y., Wang, Y.Y., and Wong, F.S., "Assessment of Liquefaction Potential Using Neural Networks," *Soil Dyn. Earthq. Eng.*, Vol. 12, No. 6, pp. 325-333 (1993).
23. Ullidtz, P. and Coetzee, N.F., "Analytical Procedure in Nondestructive Testing Pavement Evaluation," *Transport. Res. Rec. 1482*, pp. 61-66 (1995).
24. U.S. Department of Transportation, Federal Aviation Administration, *Use of Nondestructive Testing in The Evaluation of Airport Pavement* (FAA/AC 150/5370-11B), Washington, DC (2003).
25. Weil, G.J., "Non-destructive Testing of Bridge, Highway and Airport Pavements," *Geol. Surv. Finland*, Vol. 16, pp. 259-266 (1992).
26. Yang, C.H., Wang, C.Y., and Ko, C.M., "Detecting the Structure of Flexible Pavement Using Ground Penetrating Radar," *NDT Sci. Technol.*, Vol. 18, No. 2, pp. 44-53 (2000). (in Chinese)